Journal of Physics: Conference Series

PAPER • **OPEN ACCESS**

Load-shifting strategies in district heating networks with constant supply temperature: the case study of Verona

To cite this article: J Vivian *et al* 2020 *J. Phys.: Conf. Ser.* **1599** 012038

View the article online for updates and enhancements.

You may also like

- Multistrip synthetic single-crystal-diamond photodiode based on a p-type/intrinsic/Schottky metal transverse configuration
  I. Ciancaglioni, Marco Marinelli, E. Milani et al.
- Advances in SAW-based gas sensors
  C Caliendo, P Verardi, E Verona et al.
- Single-crystal diamond detector for time-resolved measurements of a pulsed fast-neutron beam
  A. Pietropaolo, C. Andreani, M. Rebai et al.

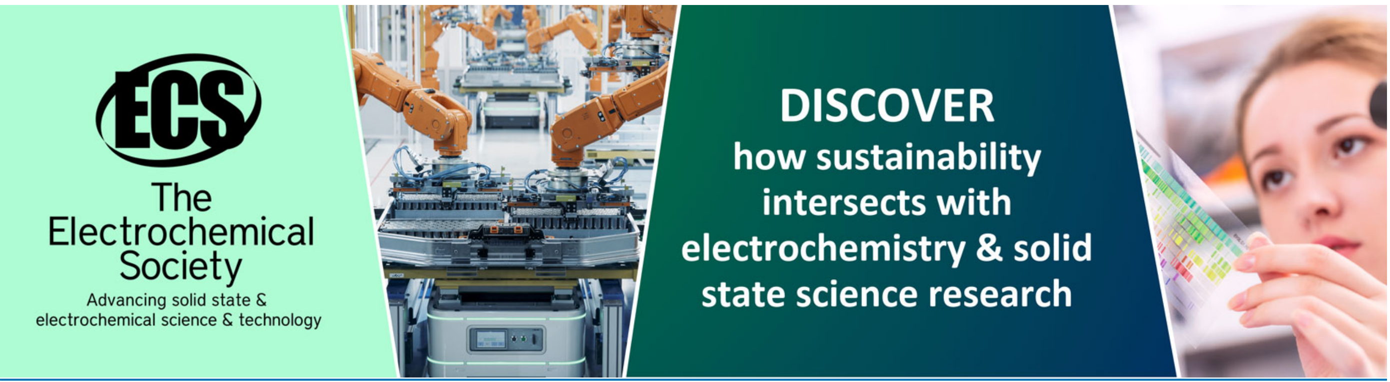

This content was downloaded from IP address 18.119.192.55 on 15/05/2024 at 04:24

Load-shifting strategies in district heating networks with constant supply temperature: the case study of Verona

J Vivian[1], D Quaggiotto[1], E Ploner[1], F D'Isep[1], A Zarrella[1]

[1] DII, University of Padova - via Venezia 1, 35131 Padova (Italy)
Corresponding author e-mail: davide.quaggiotto@phd.unipd.it

Abstract. District heating and cooling networks are a key infrastructure to decarbonise the heating and cooling sector. Besides the design of new networks according to the principles of the 4th and 5th generation district heating, operational aspects may significantly contribute to improve the efficiency of existing networks from both economic and environmental standpoints. In the present work, computer simulations using a district heating network model (NeMo) were carried out to investigate the load shifting potential offered by the thermal capacitance of the water volume enclosed in the network pipelines. The average return temperature is increased before the occurrence of the peak load by adjusting the flow rate according to the forecasted heat demand for the upcoming hours. The effectiveness of this control strategy was demonstrated for the district heating network of Verona, proving that the peak load can be significantly reduced, especially during middle season. Finally, the load shifting strategy was used to allow a change in the heat production mix, thereby reducing the primary energy consumption of the main heat supply station during the considered period.

1. Introduction

District heating (DH) networks play a key role in the transition towards sustainable cities, thanks to their ability to efficiently provide space heating and domestic hot water to buildings through the use of renewable sources -such as geothermal and solar energy- waste heat sources and cogeneration plants. Since almost half of the final energy use in Europe is related to heating services, the construction and the expansion of efficient DH systems are among the key points of European energy policy [1]. Lund et al. [2] developed the concept of low temperature district heating (LTDH), or 4th generation district heating (4GDH). The basic idea behind it is the reduction of the supply temperature to abate distribution heat losses and to allow low-grade heat sources such as renewables and low temperature waste heat to be integrated in the network. The evolution of DH systems towards the 4th generation has been driven by the reducing trend of heat demand that is expected to continue during next decades due to the progressive refurbishment of existing buildings and to the high energy performance of new buildings. Demonstration projects carried out in different locations have proved the effectiveness and the competitiveness of low temperature district heating systems for both new low energy buildings [3] and existing buildings [4]. In the last decade around 40 DHC systems of the so-called 5th generation were put in operation: the heat carrier of these networks is below 45°C (minimum temperature required for DHW production) and they can fulfil both the heating and cooling demands of buildings by means of distributed heat pumps installed at the customer substations [5]. In a previous study, the advantages of these networks and their sensitivity to the main design parameters were investigated for a heating-only case-study [6]. Besides planning, design and business aspects, the control of both new and existing

Content from this work may be used under the terms of the Creative Commons Attribution 3.0 licence. Any further distribution of this work must maintain attribution to the author(s) and the title of the work, journal citation and DOI.
Published under licence by IOP Publishing Ltd

networks can significantly improve their economic and environmental performance. To this end, researchers have proposed different control strategies for the optimal management of the supply and demand sides of the network, including load shifting strategies and scheduling of the heat generators based on look-ahead optimization problems. For instance, Guelpa et al. [7] used a physical simulation model to minimize the primary energy consumption of the thermal plants by reducing the thermal peak request of the Turin district heating network. Other researchers developed model predictive controllers to determine the optimal supply temperature of DHNs –see e.g. [8]. Several district heating network models have been proposed by the scientific community. Most of them are based either on the node method or on finite-difference methods [9]. A steady-state hydraulic and transient thermal model, called NeMo, has been developed by University of Padova to reproduce the hydraulic and thermal behaviour of district heating and cooling networks. NeMo resembles the model proposed by Polytechnic of Turin, which was used for studying both thermal [7] and hydraulic [10] behavior of complex thermal networks. In a previous paper a study has been conducted to investigate the accuracy of the model, based on a finite difference scheme, in reproducing the heat waves along a single pipe. The study proved that the heat propagation throughout the network can be accurately reproduced, provided that the network is correctly discretized [11]. The study revealed that the discretization giving the best output depends on the time-step of the internal solver and on the Courant number. The current study set out to use NeMo to simulate the thermal and hydraulic behavior of a real urban district heating network investigating the feasibility of control strategies aimed at shifting the heat load according to the needs of the DH operator. The heat capacity of the water enclosed in the network pipelines is used to decouple the heat load profile at the supply station from the heat demand of the users substations. The paper specifically targets load shifting strategies for networks with constant supply temperature and variable flow rate.

2. Model

The district heating network model NeMo has been already described in the aforementioned paper [11]. The topology of the network is described by using graph theory. The network is represented by a set of nodes and oriented branches and an adjacency matrix determines their mutual connections. Once the geometry is established, the pressure and temperature profiles are calculated. When forced convection occurs, the velocity of the heat carrier fluid does not depend on the temperature distribution. Therefore, the hydraulic and thermal sub-models can be uncoupled. This allows the calculation of the mass flow rates and the pressures across the network in a first step; then, given the mass flow rates, the energy balance is performed to find out the temperature distribution. The model assumes a slug flow (one dimensional model) and neglects both the heat conduction in the axial direction and the heat capacity of the surrounding ground. The heat transfer in the radial direction considers the convection between the heat carrier fluid and the inner pipe surface, the thermal insulation of the pipe and the thermal resistance of the surrounding ground. Due to the uncompressible nature of the heat carrier fluid, the hydraulic problem can be described using only two equations: the continuity and the momentum equations. NeMo solves these equations using the SIMPLE method proposed by Patankar and Spalding [12]. The heat propagation in the network is then described by the energy balance performed on the volume of heat carrier fluid around the nodes of the network. The control volume of the i-th node corresponds to half of the heat carrier fluid volume of all the branches connected to it.

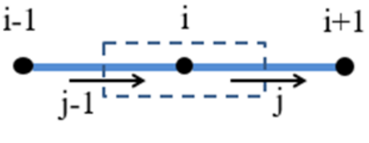

Figure 1. Control volume of the i-th node.

Applying the energy balance to the node shown in Figure 1 leads to Equation (1):

$$\rho \mathrm{V_i} \mathrm{c_p} \frac{\partial \mathrm{T_i}}{\partial \tau} = G_{j-1} c_p T_{j-1} - G_j c_p T_j - \frac{1}{2} \left(\mathrm{L_j} \Omega_\mathrm{j} U_j + \mathrm{L_{j-1}} \Omega_\mathrm{j-1} U_{j-1} \right) (\mathrm{T_i} - \mathrm{T_\infty}) \qquad (1)$$

Where G are the mass flow rates, V is the volume of heat carrier fluid enclosed in the control volume, Ω is the perimeter of the pipe section, U is the radial heat transmission coefficient from fluid to the ground and T_∞ is the undisturbed ground temperature. The temperature of the branches is then associated to the temperature of the corresponding upwind nodes, according to the well-known upwind scheme. Therefore, Equation (1) becomes:

$$\rho V_i c_p \frac{T_i^{(\tau)} - T_i^{(\tau-\Delta\tau)}}{\Delta\tau} = G_{j-1} c_p T_{i-1}^{(\tau)} - G_j c_p T_i^{(\tau)} - \frac{1}{2}\left(L_j \Omega_j U_j + L_{j-1}\Omega_{j-1}U_{j-1}\right)\left(T_i^{(\tau)} - T_g\right) \tag{2}$$

Equation (2) can be represented in matrix form as:

$$M\,\dot{T} = q - K\,T \tag{3}$$

Where M and K are the so-called mass matrix and stiffness matrix, respectively. The temperature at the inlet node is fixed (Dirichlet condition). The first-order ordinary differential equation (ODE) (3) is solved by Matlab's ODE solver ode15s that implements the Numerical Differentiation Formulas [13].

3. Case study

The case study under consideration is the district heating network of Verona Centro Città, shown in Figure 1. The network extends for a length of about 25 km, providing heat for space heating and -in some cases- domestic hot water to 247 users. The users supplied have a total volume of about 3.2 Mm^3 and need about 70 GWh/year of heat, with a peak load of approximately 38 MW.

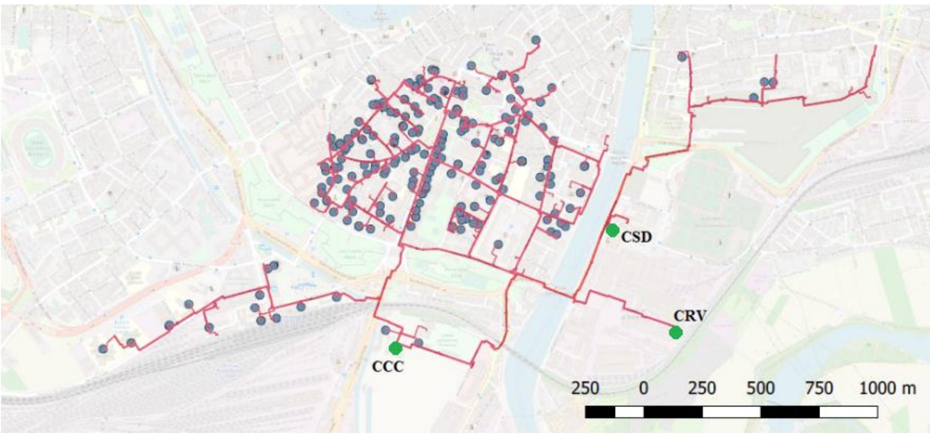

Figure 2. Plan of the district heating network of Verona Centro Città obtained with QGis [14].

The blue dots in Figure1 represent the substations of the users, while the three green dots correspond to the supply stations. The main one is CCC, that supplies heat produced by five CHP units, heat pumps (supplied by the cooling circuit of the CHP) and three auxiliary gas boilers; CRV recovers heat from a foundry and CSD has other three auxiliary and reserve gas boilers. CRV can always supply heat to the network, when available from the industrial process.

Table 1. Installed thermal and electrical power of the supply stations.

Station		Units	Total installed power
CCC	CHP: gas-fired internal combustion engines	5	11 MW_t (11.25 MW_e)
	HP: heat pumps	5	2.0 MW_t
	GB: gas boilers	3	25.5 MW_t
CRV	WH: waste heat from foundry	1	1.1 MW_t
CSD	GB: gas boilers	3	3.4 MW_t

The DH network operates with a constant supply temperature (80°C in winter, 75°C in summer) and variable mass flow rate. A rule-based control has been implemented and fine-tuned over the years to prevent discomfort problems due to low mass flow circulation and to keep the temperature difference between supply and return pipe at the main supply station around 20 K.

4. Method

As suggested by Van der Hejide et al. [15], it is possible to consider representative periods which adequately mimic the district heating behaviour for the entire year. Two representative weeks were chosen to study the load shifting strategies: a cold winter week with an average heat load of 14.1 MW_t and a week during middle season with an average heat load of 4.8 MW_t. In the first case all five ICEs supply heat to the network, whereas in the spring week only one or two engines are switched on. The approach followed in the present work consisted in simulating the thermal and hydraulic behavior using NeMo in the two representative weeks with current and modified pumping strategy. The same heat load profiles at the users substations have been imposed. The resulting heat load profiles at the main supply station (CCC) were compared to the reference ones using the indicators listed in section 4.2.

4.1 Simplification of network topology

The network shown in Figure 1 and described in the previous Section has been simplified in order to reduce the computational effort needed to run the simulation. Table 2 shows the difference between the original data and the final model used in the study. We assumed that all the heat is supplied by station CCC. This choice was taken to better analyze the correlation between mass flow rate and heat load profile at the supply station, without "disturbance" due to mass flow injected from distant supply points.

Table 2. Topological difference between real network and model.

Parameter	Real network	Model
Number of substations	247	65
Number of heat supply points	3	1
Number of nodes	>1000	150
Number of branches	>1000	159
Loops	11	11

4.2 Load shifting strategy

The current pumping strategy is based on the experience of the DH operator. The pressure head provided by the pumps guarantees a minimum pressure difference at the critical substation. In this paper, this pumping strategy is modified, when convenient for the DH network operator, using the network as a heat storage system. The average network temperature is used as an indicator of the *state-of-charge* of the storage system. Circulating more/less water in the network leads to a drop/increase in the temperature difference between supply and return pipe. Therefore, the mass flow rate must be increased/decreased compared to the current pumping strategy in order to charge/discharge the network. The idea is to regulate the mass flow rate based on the heat load predictions for the next hours. Five dimensionless parameters determine the mass flow rate profile for the next hours, as shown in Figure 3.

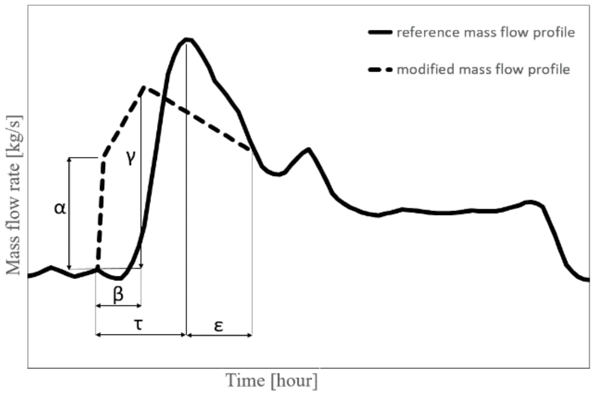

Figure 3. Parameters used to evaluate the variation of mass flow rate.

Parameters τ and ε define the time interval in which the mass flow profile will deviate from the reference one before and after the peak load, respectively. The remaining three parameters (α, β and γ) determine the shape of the mass flow profile, so they can be define shape parameters. Numerous simulations have been carried out, considering different combinations of the parameters α, β and γ, varying one parameter at a time and with τ and ε constant. To limit the number of results to show, the three combinations of shape parameters, that gave the best peak shaving results, were chosen, as shown in Table 3. To compare C1, C2, C3, for each of these, parameter τ has been varied considering the values 1.5, 2.5, 3.5 and 4.5 hours. Overall, 24 weekly simulations (12 simulations for each of the two references weeks) have been selected to prove what kind of advantages and disadvantages the regulation strategies of the flow rate involve. For all these simulations the parameter ε = 3 hours was kept constant.

Table 3. The three considered combinations of parameters α, β and γ.

Combinations	α	β	γ
C1	0.2	0.5	0.8
C2	0.1	0.1	0.9
C3	0.7	0.5	0.7

4.3 Evaluation of the load shifting potential

In order to determine the impact of such a regulation on the operation of the network in relation to the current situation, a number of indicators have been defined. The first indicator, ΔQ_t, indicates the variation of thermal energy supplied by the plant compared to the reference simulation:

$$\Delta Q_t = \frac{Q_{t,mod} - Q_{t,ref}}{Q_{t,ref}} \tag{4}$$

Likewise, ΔW_{el} measures the variation in electrical energy required for pumping compared to the reference case. The indicator Δq_{max} in Eq. (5) indicates the damping of the thermal load peak at the power plant with the modified pumping strategy, while $\Delta t_{q_{max}}$ –Eq. (6)- indicates its time shift. Negative values indicate an anticipation of the peak, while positive values indicate a delay in the phase shift with respect to the reference case.

$$\Delta q_{max} = \frac{q_{max,ref} - q_{max,mod}}{q_{max,ref}} \tag{5}$$

$$\Delta t_{q_{max}} = t_{max,mod} - t_{max,ref} \tag{6}$$

A discomfort index called PD_{rel} has been calculated as reported in Eq. (7) to assess whether the control method applied to the district heating network could lead to lower the quality of service to the users. It was assumed that the probability of causing discomfort is roughly proportional to the decrease of the return temperature at the user nodes for the entire duration of the control.

$$PD_{rel} = \begin{cases} \int_0^{168} \left(T_{r,ref} - T_{r,mod}\right) dt, & T_{r,ref} > T_{r,mod} \\ 0 & T_{r,ref} \leq T_{r,mod} \end{cases} \tag{7}$$

5. Results

5.1. Load-shifting potential in two representative weeks

The results in Table 4 have been obtained with the same combination of the parameters α, β, and γ, i.e. with the same shape of the modified flow profile, while the parameter τ has been varied from 1.5 to 4.5 hours. The combination C1 was chosen because it results in the least marked variation compared to the original profile. As the value of τ increases from 1.5 to 4.5 hours, all the considered indicators progressively increase. As far as the energy-related indicators are concerned, the thermal energy needs ΔQ_t increases from 0.14% to 0.30% in February, whereas the variation is almost negligible in April. The

IOP Publishing
1599 (2020) 012038 doi:10.1088/1742-6596/1599/1/012038

energy needs for pumping ΔW_{el} increases from -5.2% to +4.6% in February and from -1.3% to 1.5% in April. The peak load reduction Δq_{max} shows a limited increase in February (approximately from 9% to 10%) and a significant increase in April (from 4% to 17%). Such peak shaving is almost proportional to the time shift of the peak load. The peak is always delayed in February, whereas there is a significant change in April, when the peak is anticipated with $\tau = 1.5$ hours and delayed for τ higher than 2.5 hours. As it can be seen the power peak of the reference profile is replaced by two smaller peaks in the modified power profile, one in advance and one in delay.

Table 4. Effect of τ on performance indicators.

τ [h]	$q_{max,mod}$ [MW]		Δq_{max} [%]		Δt_{max} [%]		ΔQ_t [%]		ΔW_{el} [%]		PD_{rel} [°C h]	
	FEB	APR	FEB	APR	FEB	APR	FEB	APR	FEB	APR	FEB	APR
1.5	22.96	6.56	8.9	4.2	0.67	-0.67	0.14	-0.02	-5.2	-1.3	11	4
2.5	22.74	6.15	9.7	10.1	0.75	-1.17	0.19	-0.01	-4.0	-1.3	14	6
3.5	22.66	5.79	10.0	15.4	0.83	0.50	0.26	0.04	0.2	-0.1	16	7
4.5	22.63	5.69	10.1	16.9	0.83	1.50	0.30	0.08	4.6	1.5	17	7

The peak in advance is the result of the rapid increase of flow rate imposed by the new control strategy, whereas the peak in delay originates from the heat demand profile of the users. According to the parameters combination, the average velocity of the heat transfer fluid and the thermal load profile, one of the two peaks prevails. Moreover, increasing τ from 1.5 h to 4.5 h brings to an increase of the discomfort index by 50% in February and to double it in April.

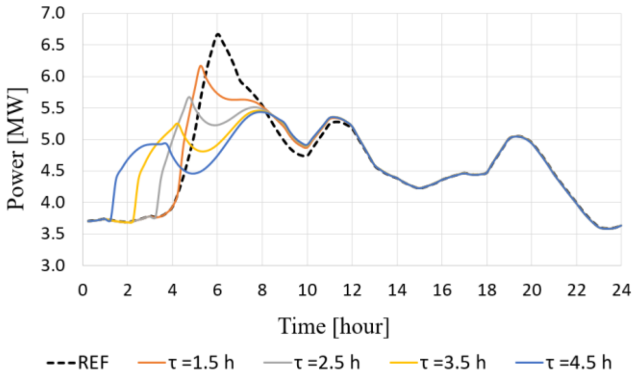

Figure 4. Power profiles obtained by varying τ on Tuesday, April week.

Table 5 shows the effect of the different combinations (C1, C2 and C3) on the performance indicators for a given τ –the intermediate value of 2.5 hours was chosen. The results refer to two typical days: a working day (Tuesday) and a weekend day (Sunday). Table 5 shows that in February the peak is always postponed except for Sunday with the combination C2, i.e. when the heat load is lower and with the sharpest mass flow rate increase.

Table 5. Effect of the different combinations on the performance indicators with τ =2.5.

Month – Comb.	$q_{max,mod}$ [MW]		Δq_{max} [%]		Δt_{max} [%]		ΔQ_t [%]		ΔW_{el} [%]		PD_{rel} [°C h]	
	TUE	SUN	TUE	SUN	TUE	SUN	TUE	SUN	TUE	SUN	TUE	SUN
FEB – C1	23.53	18.08	8.5	12.4	0.75	1.0	0.18	0.19	-4.0	-2.0	14	14
FEB – C2	23.48	18.24	8.7	11.6	0.75	-2.25	0.11	0.14	0.4	1.8	14	14
FEB – C3	23.53	18.08	8.5	12.4	0.75	1.25	0.13	0.16	-3.5	-1.5	18	17
APR – C1	5.68	6.23	14.9	6.9	-1.25	-2.5	0.02	-0.01	0.02	-1.5	5	6
APR – C2	6.42	6.90	3.8	-3.1	-2.25	-1.00	0.06	-0.02	1.41	-2.01	4	6
APR – C3	5.88	6.42	11.9	4.1	-2.50	-2.00	0.04	-0.01	0.35	-1.30	6	7

These two conditions together lead the first power peak to exceed the second, as it can be seen in Figure 5(b). In April, the same condition leads to increase the thermal peak load of the network of approximately +3% compared to the reference control strategy. With all the considered combinations, the discomfort index during February is always higher than in April. The same trends hold true in case the flow rate adjustment starts earlier, such as in the case τ=4.5 h. In April, the comparison between the different combinations shows that C1 is definitely the best choice in order to damp the daily power peak. If there is no need to damp the power peak, with the combinations C2 and C3 it is possible to obtain a marked translation in advance of the reference power peak.

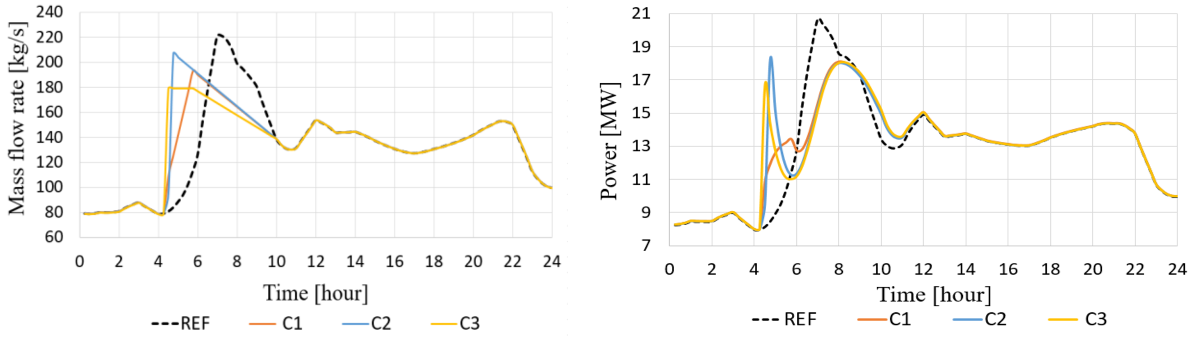

Figure 5. Different shapes of the modified (a) flow rate and (b) heat load profiles connected to the combinations C1, C2, C3 for Sunday, week of February.

5.2 Assessment of the primary energy-saving potential

The thermal load profile can be flattened thanks to the new control strategy that uses the network as a storage. This allows to reduce the share of heat produced by the gas boilers and to increase the share covered by the heat pumps and the CHP, which guarantees a drop in the primary energy consumption compared to the separate production of heat and power. Considering the middle season representative week, the C1 pumping strategy with τ=4.5 hours determines the best peak shaving results. Applying this strategy the heat productions covered by the CHP and by heat pumps increase respectively of 1.2% and of 0.9%, while that one supplied by gas boilers decrease of 2.1% -see Figure 6. Consequently, the primary energy consumption can be reduced by 7.75 MWh (1.5%), equivalent to 1.4 t_{CO2} in one week.

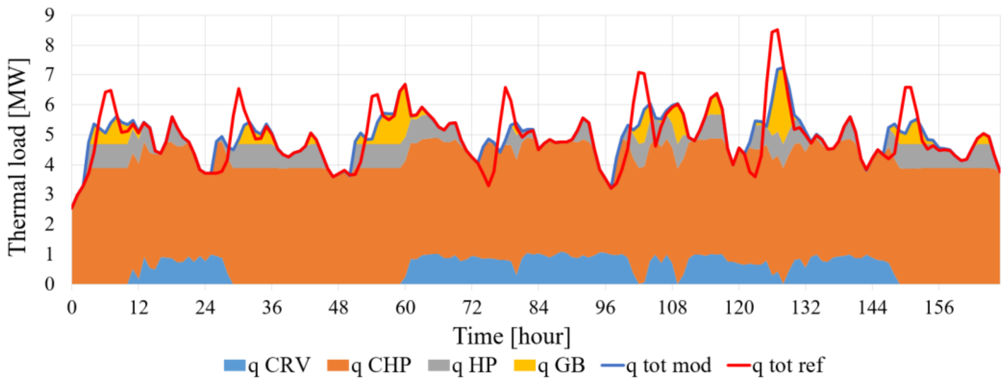

Figure 6. Reference and modified thermal load profiles and energy supply mix in April week.

6. Conclusions

In this article, the district heating network model NeMo was used to reproduce the dynamic behaviour of the district heating network of Verona. Several simulations were carried out for two representative weeks, with different pumping strategies aimed at reducing the thermal power peak and shifting the heat load in time. Three dimensionless parameters and two temporal parameters allowed the construction of modified mass flow rate profiles depending on the heat load forecast for the next hours. The simulation results showed that a combination of parameters that involves a gradual increase of flow rate before the peak load is able to achieve an average peak shaving of 10% in February and 12 % in April. According to the aforementioned parameters, the thermal peak load is both reduced and temporally shifted, in advance or in delay compared to reference heat load profile. The paper shows that this behaviour depends on how the flow rate variations influence the charge and discharge cycles of network. Furthermore, a pre-charge strategy of network was applied to the week of April to reduce the primary energy consumption. Indeed, flattening the heat load profile at the main supply station allows to increase the share of CHP and heat pumps in the energy production mix and to reduce natural gas consumption of boilers. In conclusion, the study proves that the thermal capacitance of district heating networks allows to shift consistently the energy production especially during middle seasons.

Acknowledgements
The research activities of D. Quaggiotto and J. Vivian were funded by the Regional Project GHOTEM (POR-FESR 2014-2020, ID 10064601) and by the BIRD 2017 program promoted by the University of Padova (BIRD177824), respectively. The authors would like to thank the District Heating operator of Verona (AGSM SpA) for the fruitful discussions and for sharing their knowhow and the monitored data.

References
[1] "Directive 2010/31/EU of the European Parliament and of the Council of 19 May 2010 on the energy performance of buildings," 2010.
[2] H. Lund *et al.*, 2014 "4th Generation District Heating (4GDH): Integrating smart thermal grids into future sustainable energy systems," *Energy* 68, pp. 1–11.
[3] A. Dalla Rosa and J. E. Christensen, 2011, "Low-energy district heating in energy-efficient building areas," *Energy* 36 (12): 6890–99.
[4] M. Brand and S. Svendsen, 2013, "Renewable-based low-temperature district heating for existing buildings in various stages of refurbishment," *Energy* 62: 311–319.
[5] S. Buffa, M. Cozzini, M. D'Antoni et al. 2019 "5th generation district heating and cooling systems: A review of existing cases in Europe" *Renew. And Sust. Energy Reviews* 104: 504-22
[6] J. Vivian, G. Emmi, A. Zarrella et al., 2018 "Evaluating the cost of heat for end users in ultra low temperature district heating networks with booster heat pumps" *Energy* 153: 788-800.
[7] E. Guelpa, G. Barbero, A. Sciacovelli et al, 2017, "Peak-shaving in district heating systems through optimal management of the thermal request of buildings," *Energy* 137: 706–14.
[8] R. Bavière and M. Vallée, 2018 "Optimal Temperature Control of Large Scale District Heating Networks," *Energy Procedia* 149: 69–78.
[9] H. Palsson, 2000, Methods for planning and operating decentralised combined heatand power plants. PhD Thesis. Riso National Laboratory, Roskilde (Denmark).
[10] E. Guelpa, C. Toro, A. Sciacovelli et al., 2016, "Optimal operation of large district heating networks through fast fluid-dynamic simulation," *Energy* 102: 586–95.
[11] J. Vivian, P. M. Á. de Uribarri, U. Eicker et al., 2018, "The effect of discretization on the accuracy of two district heating network models based on finite-difference methods," *Energy Procedia* 149: 625–34.
[12] S. Patankar and D. Spalding, 1972, "A calculation procedure for heat, mass and momentum transfer in three-dimensional parabolic flows," *Int. J. Heat Mass Transf.* 15 (10), 1787–1806.
[13] L. F. Shampine LF, M.W. Reichelt. The MATLAB ODE Suite. *SIAM Journal on Scientific Computing* 1997;18:1–22.
[14] QGIS Development Team (2019). QGIS Geographic Information System. Open Source Geospatial Foundation Project. http://qgis.osgeo.org.
[15] B. van der Heijde, A. Vandermeulen, R. Salenbien, L. Helsen, 2019, "Representative days selection for district energy system optimisation: a solar district heating system with seasonal storage." *Applied Energy* 248: 79-94.